

esa SP - 359

March 1993

Volume II

Proceedings of the First ERS-1 Symposium

**SPACE AT THE SERVICE OF OUR
ENVIRONMENT**

4 - 6 November 1992
Cannes, France

european space agency / agence spatiale européenne
8-10, rue Mario-Nikis, 75738 Paris Cedex 15, France

Organising Committee

Chairman G. Duchossois, ESA, Paris, France

Members S. Bruzzi, ESA, Paris, France
E. Attema, ESTEC, Noordwijk, The Netherlands
J. Benveniste, ESRIN, Frascati, Italy
R. Francis, ESTEC, Noordwijk, The Netherlands
J.P. Guignard, ESTEC, Noordwijk, The Netherlands
H. Laur, ESRIN, Frascati, Italy
J. Louet, ESTEC, Noordwijk, The Netherlands
E. Loeffler, ESRIN (visual displays), Frascati, Italy
C. Tapp, ESA, Paris, France
B. Kaldeich, ESA Editor, ESTEC, Noordwijk, The Netherlands

Published by: *ESA Publications Division*
ESTEC, Noordwijk, The Netherlands

Editor: *Brigitte Kaldeich*

Price: *Dfl 150.00 (2 volumes)*

ISBN 92-9092-278-8

© 1993 European Space Agency

Cover illustration shows shaded elevation model of Greenland, produced from ERS-1 Fast Delivery Radar Altimeter Data (courtesy Mullard Space Science Laboratory)

ON THE EXTRACTION OF OCEAN WAVE SPECTRA FROM ERS-1 SAR WAVE MODE IMAGE SPECTRA

C. Brüning¹, S. Hasselmann², K. Hasselmann², S. Lehner², T. Gerling³

¹Institut für Meereskunde, Universität Hamburg;

²Max-Planck-Institut für Meteorologie, Hamburg;

³Applied Physics Lab., The Johns Hopkins University

Abstract

The ERS-1 synthetic aperture radar (SAR) wave mode data contain valuable global information on the full two-dimensional ocean wave spectrum. This must be extracted, however, from non-linearly distorted images. Wave spectra were derived from SAR wave-mode image spectra using Hasselmann's inversion scheme based on their closed nonlinear spectral integral transform relation describing the mapping of a wave spectrum into a SAR image spectrum. The scheme uses a first-guess (WAM) model wave spectrum as regularization term. The optimally fitted wave spectra yield simulated SAR image spectra in good agreement with measured SAR spectra. The wave spectra provide significant wave heights to the same accuracy as ERS-1 radar altimeter. The separation of the SAR-derived wave spectra into individual wave systems using a partitioning technique showed excellent overall agreement with modelled wave spectra while demonstrating the complexity of typical wave spectra in the open ocean.

Keywords: SAR ocean wave imaging

1 Introduction

The Active Microwave Instrument (AMI) aboard the First European Remote Sensing Satellite ERS-1 includes a C-band synthetic aperture radar (SAR) which can operate in so called Wave Mode. In contrast to the full-swath SAR, this is able to provide global wave data in the form of 10 km x 5 km SAR images (imagettes) sampled every 200 km along the satellite track. The following paper represents a first attempt to validate these data in a quasi-operational setting.

The theory of the SAR imaging of ocean waves is basically well understood (Refs. 1,2,3,4). The mapping of an ocean wave spectrum into a SAR image spectrum is a complex, in general strongly nonlinear process. However, with the derivation of nonlinear spectral transform relation in closed form by Hasselmann and Hasselmann (Ref. 5 cf. also Ref. 6) it has become possible to compute the forward transformation and its inverse within the computational constraints of operational applications. The inversion is solved iteratively by making use of the explicit inversion for an approximate, quasi-linear form of the transform relation. The SAR-derived wave spectra are calibrated internally, independently of the SAR calibration or

direct measurements of the mean cross-section, by relating the wave-modulation spectrum to the simultaneously measured background clutter noise spectrum (Refs. 7,8).

The inversion scheme requires first-guess wave spectra to remove the 180° ambiguity inherent in all frozen-surface image spectra. These are provided in the present study by the operational 3° x 3° global wave model WAM (Ref. 10) of the European Centre for Medium Range Weather Forecasts (ECMWF). Parallel integrations with a 1° x 1° WAM model for the Atlantic carried out at the Max Planck Institute of Meteorology (MPI) in Hamburg yielded only small differences compared with the lower resolution global runs (Ref. 13). In both models the frequency resolution was 10% on a logarithmic frequency scale, while the angular resolution was 30° and 15°, respectively, for the global and Atlantic versions of the model. Both models were driven by the ECMWF operational 1/2° x 1/2° wind fields.

SAR variance spectra calculated from imagettes provided in Fast Delivery Format by ESTEC were used to derive wave spectra. Typical examples of WAM first-guess and fitted ocean wave spectra, simulated and measured SAR image spectra, are shown for Sept. 1992. Each wave system is separated by a 'partitioning' scheme (Ref. 9) derived from first-guess and optimally fitted wave spectra which allow the identification of wave field errors. Furthermore, global and regional monthly statistics of significant wave height obtained between Sept. 1 - 30, 1992, demonstrate the high accuracy and good performance of the SAR ocean wave inversion scheme.

2 SAR Wave Mode Data

Following a pilot study using data obtained for January 22-24, 1992 (Ref. 8), about 60,000 global ERS-1 SAR wave mode imagette spectra have been analysed on a continuous basis between July and October 1992. Variance spectra were calculated from imagettes consisting of 320 pixels in azimuth (flight direction) and 600 pixels in ground range direction. The pixel size is 16 m in azimuth and 20 m in ground range. The cartesian SAR image spectra were transformed into polar coordinates and smoothed on a reduced spectral grid of 12 logarithmically spaced wavenumbers between 100 m - 1000 m (corresponding to 20% resolution, or 10% frequency resolution) and 12 directions (corresponding to 15° resolution for the symmetrical frozen-image spectrum). Since the official

SAR wave mode spectral Fast Delivery Product was not yet reliable, the spectra were made available in an off-line mode directly from ESTEC for further analysis at MPI.

3 The SAR Imaging Model and its Inversion

The standard theory of SAR ocean wave imaging is based on a two-scale Bragg scattering model. The imaging processes consist of tilt and hydrodynamic modulation, and range and velocity bunching (Refs. 1,2,3,4,5,8,11). Tilt, hydrodynamic, and range-bunching modulation can be represented to first order as linear processes characterized by modulation transfer functions. These can be collected into a net real aperture radar (RAR) modulation transfer function. Velocity bunching, however, is a pure SAR, inherently nonlinear imaging process caused by the long-wave orbital motion of the sea surface.

In Hasselmann's SAR imaging theory, the Gaussian statistics of the sea surface are invoked to derive a closed nonlinear integral transfer relation describing the mapping of a wave spectrum into a SAR image spectrum. The relation can be rapidly evaluated by expanding in a Fourier transform series.

The inversion of the transform relation is based on a maximum likelihood method in which a cost function representing the error between the observed and simulated SAR image spectra is minimized. The deviation of the wave spectrum from a first-guess spectrum is included in the cost function as an additional regularization term to overcome the SAR-inherent 180° ambiguity. The inversion is solved iteratively by alternating fully nonlinear forward transformations with

approximate inverse transformations based on a quasi-linear truncated form of the forward transformation for which the inversion can be given explicitly.

An important feature of the SAR imaging theory is that the SAR derived wave spectra can be calibrated independently of the SAR instrument calibration using the measured clutter-noise spectrum (Ref. 7); the original analysis of Alpers and Hasselmann had to be modified to allow for the fact that for ERS-1 multi-look averaging is performed with respect to amplitudes rather than energies (Ref. 8).

The computation were carried out on a 128×128 grid in wavenumber space (k_x, k_y) , where k_x and k_y denote the wavenumber components in azimuth (flight) and ground range direction, respectively. The wavenumber grid extends from 0.2 m^{-1} to 0.003 m^{-1} corresponding to wavelengths between 32 m - 2048 m. This wavelength range extends beyond the more limited range of 100 m - 1000 m in which the ERS-1 SAR wave mode image spectra are defined, but this is uncritical, since the regularization term in the cost function ensures that the missing information is augmented by the first-guess wave spectrum.

4 Results

More than 60,000 SAR wave mode spectra were analysed for the period 1. July - 31. October 1992. First-guess model wave spectra were assigned to the ERS-1 SAR image spectra from the nearest model gridpoint and output time. In accordance with the operational system of ECMWF, output times consisted of the standard meteorological 6 hourly synoptic times.

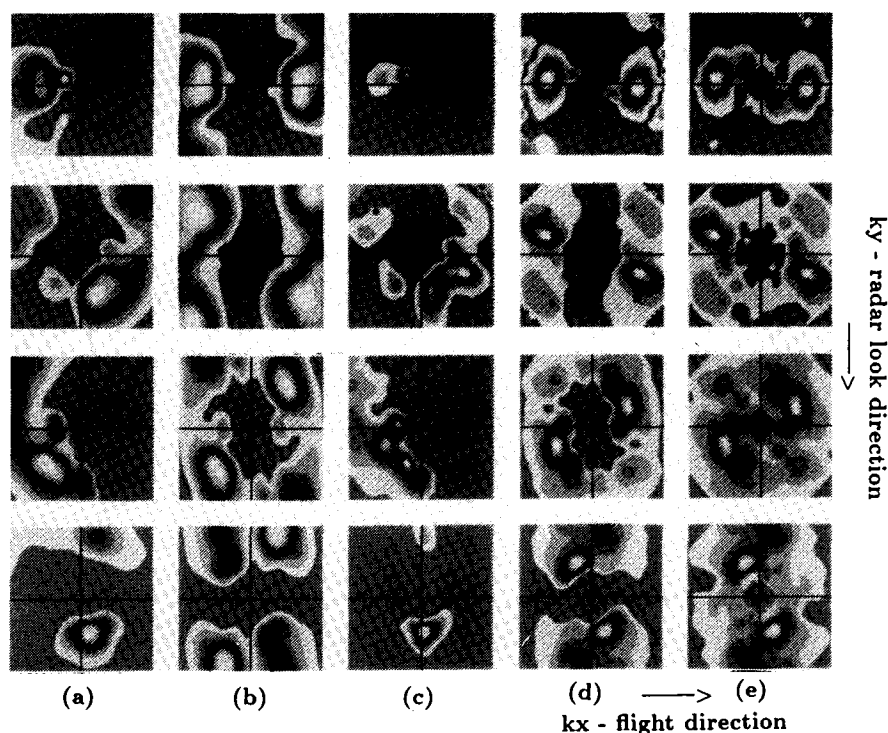


Figure 1: Examples of (a) first-guess wave spectra, (b) simulated first-guess SAR spectra calculated from (a), (c) optimally fitted wave spectra, (d) optimally simulated SAR image spectra calculated from (c), and (e) ERS-1 SAR wave mode image spectra obtained on Sept. 11, 1992. The normalized spectra are plotted in linear scale with a color-coded isoline spacing of 0.1. Here k_x and k_y are the wavenumber components in azimuth (flight) and ground range direction, respectively.

Typical examples of bi-modal wave systems propagating in azimuth (k_x) and ground range (k_y) direction are presented in Fig. 1. The spectra are normalized with respect to their maximum values and are plotted in linear scale with a color-coded isoline spacing of 0.1. Panel (a) shows the WAM first guess wave spectra, panel (b) the simulated first-guess SAR image spectra calculated from the wave spectra of Panel (a), panel (c) the extracted (i.e. optimally fitted) wave spectra, panel (d) the associated SAR image spectra calculated from the wave spectra of panel (c), and panel (e), finally, the observed SAR spectra. We note that panels (d) and (e) show excellent

agreement, indicating that the inversion method - which was designed to achieve just this agreement - was indeed successful. Furthermore, we note that although the first-guess wave spectra are in good general agreement with the optimally fitted wave spectra, the SAR data have none the less lead to recognizable modifications, demonstrating that the SAR has provided independent information beyond the information already contained in the first guess spectra - including detailed information on individual wave systems, as discussed in more detail below.

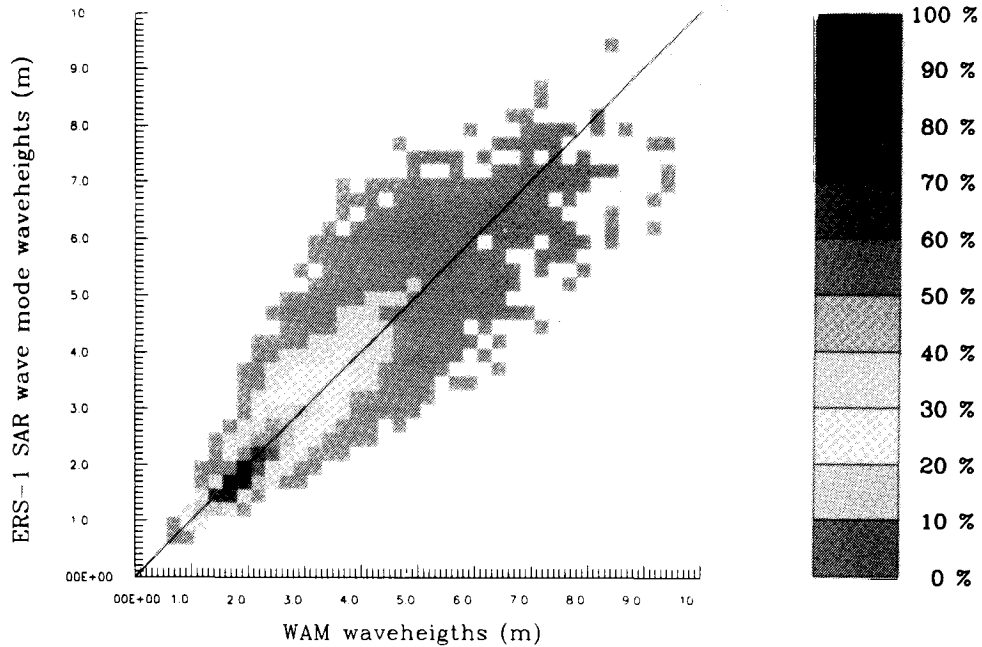


Figure 2a: Global comparison of significant wave heights computed with ECMWF WAM wave model and extracted from ERS-1 SAR wave mode image spectra, respectively, obtained during the period from Sept. 1 - 30, 1992 (15668 entries). The number of entries of individual boxes (0.25 m x 0.25 m) are color-coded. Each color represents 10% of the data.

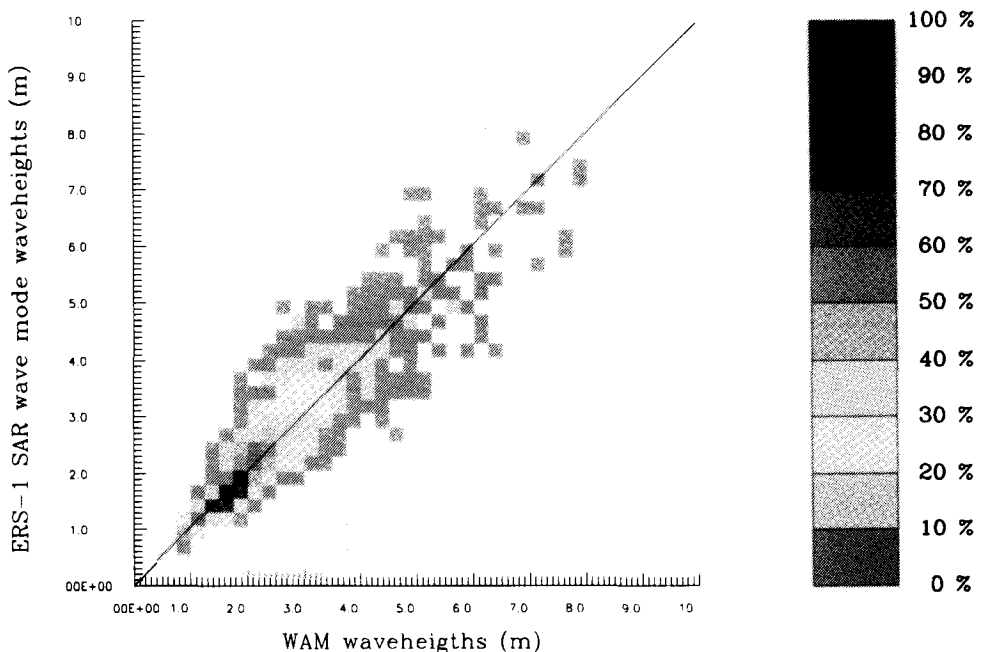


Figure 2b: Same as Fig. 2a, but for the Northern Hemisphere (20° N - 90° N).

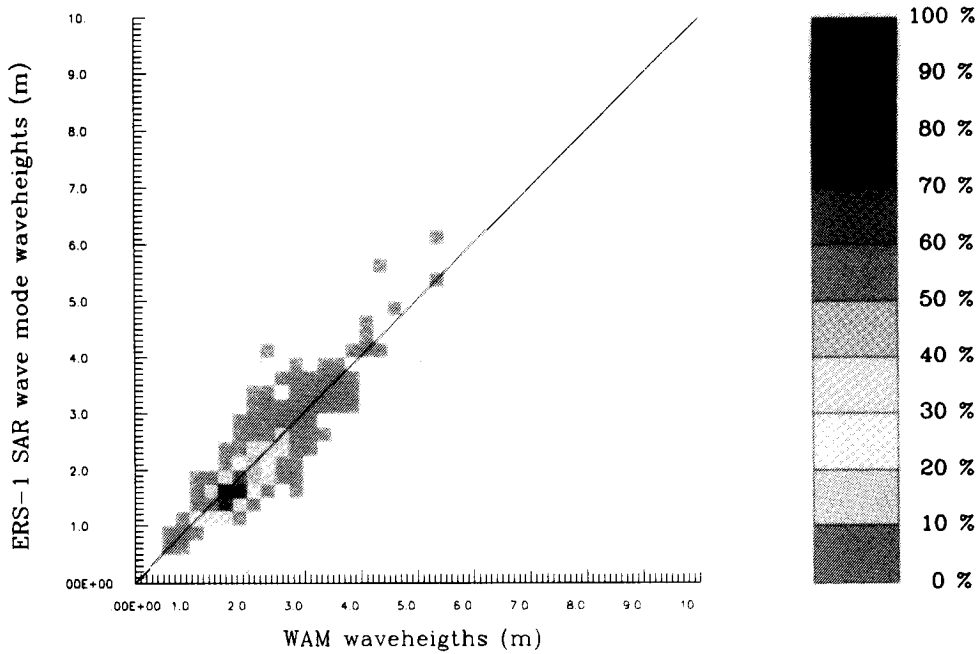


Figure 2c: Same as Fig. 2a, but for the tropics (20°S - 20° N).

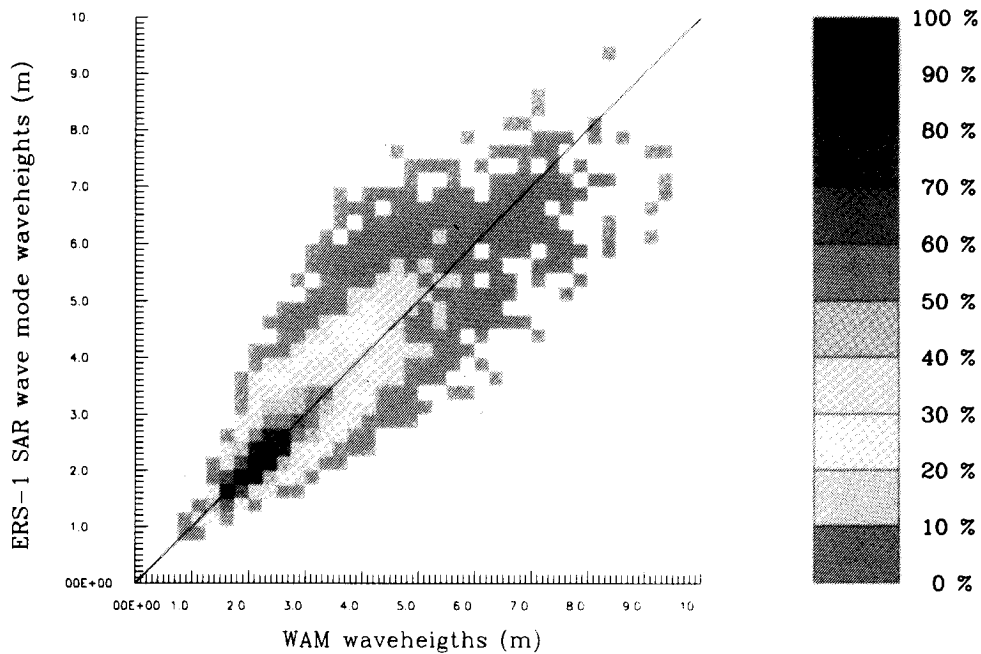


Figure 2d: Same as Fig. 2a, but for the Southern Hemisphere (20° S - 90° S).

Figs. 2 a-d compare significant wave heights obtained from the SAR derived wave spectra and from the WAM wave spectra for the month of Sept. 1992. The global comparison (panel a) is based on 15,668 entries, the regional statistics are based on 2871 entries for the Northern Hemisphere (panel b), 5,045 entries for the tropics (panel c), and 7,752 entries for the Southern Hemisphere (panel d). The number of entries of individual boxes (0.25 m x 0.25 m) are color-coded, each color representing 10% of the entries.

The overall agreement is very good and at about the same level as similar statistics for ERS-1 radar altimeter wave

height measurements (Ref. 12). The statistics for Sept. 1992 are listed together in table 1a -1d.

Table 1a
September 1992 global

ERS-1	Altimeter	SAR wave mode
Significant wave height	2.58 m	2.46 m
Bias (ERS-1 - WAM)	0.14 m	0.02 m
Standard deviation	0.48 m	0.46 m
Scatter index	0.20	0.19
Symmetric slope	1.05	1.02
Correlation coefficient	0.89	0.92

Table 1b
September 1992 Northern Hem. (excl. tropics)

ERS-1	Altimeter	SAR wave mode
Significant wave height	2.40 m	2.28 m
Bias (ERS-1 - WAM)	0.14 m	0.05 m
Standard deviation	0.46 m	0.41 m
Scatter index	0.20	0.18
Symmetric slope	1.04	1.03
Correlation coefficient	0.80	0.92

Table 1c
September 1992 tropics

ERS-1	Altimeter	SAR wave mode
Significant wave height	1.99 m	1.75 m
Bias (ERS-1 - WAM)	0.12 m	-0.09 m
Standard deviation	0.30 m	0.21 m
Scatter index	0.16	0.13
Symmetric slope	1.06	0.96
Correlation coefficient	0.72	0.90

Table 1d
September 1992 Southern Hem. (excl. tropics)

ERS-1	Altimeter	SAR wave mode
Significant wave height	3.13 m	2.98 m
Bias (ERS-1 - WAM)	0.15 m	0.08 m
Standard deviation	0.59 m	0.57 m
Scatter index	0.20	0.19
Symmetric slope	1.05	1.03
Correlation coefficient	0.87	0.89

Since SAR wave mode and radar altimeter wave heights are not measured at the same location, the data cannot be intercompared directly but only through comparison with separately collocated wave height data from the same WAM wave model. The SAR wave mode and altimeter wave heights generally exhibit a positive bias compared to the wave model data in all areas, except for the tropics, where the ERS-1 SAR wave mode data show a negative bias. It should be noted, however, that in computing the significant wave heights from the SAR derived wave spectra the integration over the high wavenum-

ber tail > 0.2 rad/m was not included. It is estimated that this lead to a small wave height under-estimation of order 0.1 m - 0.15 m.

The scatter index, the regression line slope (defined symmetrically in accordance with Ref. 12) and the standard deviation are very similar for both data sets. The correlation is generally high (0.9) except for altimeter wave heights in the tropics (0.72). The reason for this lower correlation is not known.

A comparison with integrated spectral parameters, although useful for general validation, cannot do adequate justice to the full complexity of wave spectra typically found in the open ocean. These generally consist of several wave systems emanating from different nearby or remote wind regions. To provide a more detailed intercomparison of the structures of wave spectra without entering into the analysis of the complete set of some hundred degrees of freedom of the complete model or measured wave spectra, a modified form of Gerling's spectral partitioning scheme was applied (Refs. 8,9). The wave spectrum was decomposed into a small number of principal wave systems assigned to different peaks in the spectrum. In most cases, the wave systems can be identified with different generating areas and therefore provide a concise summary of the dynamical structure and history of the wave spectrum.

Fig. 3 shows examples of the significant wave heights and propagation directions of the principal wave systems for Sept. 11, 1992 for the SAR-derived wave spectra (panel a) and collocated WAM wave spectra (panel b). The lines point in the propagation directions of the wave systems and the line lengths represent wave heights on a logarithmic scale. The overall agreement in the details of the spectral wave systems is amazingly good. Nevertheless, errors in individual wave systems can clearly be identified, especially in the Southern Hemisphere. We attribute these to wind field errors associated with sparse observations and to the fact that at this time the operational ECMWF wave model had not yet been extended to the antarctic sea ice edge but was limited by a southern boundary at 60° South.

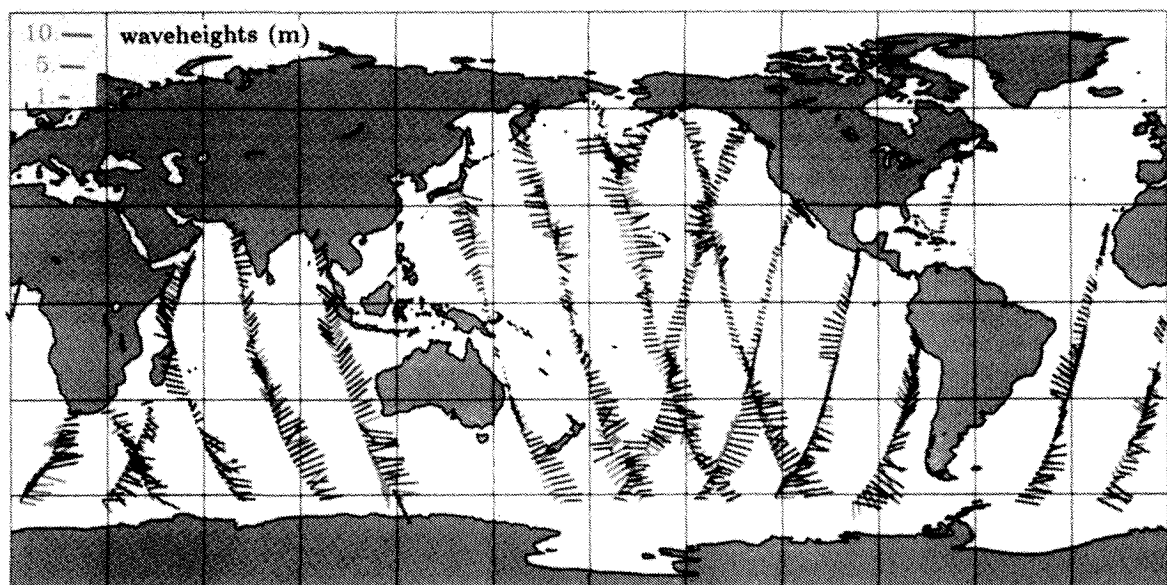


Figure 3a: Significant wave heights (in log. scale) and main propagation directions of the principal wave components obtained on Sept. 11, 1992 extracted from ERS-1 SAR wave mode image spectra.

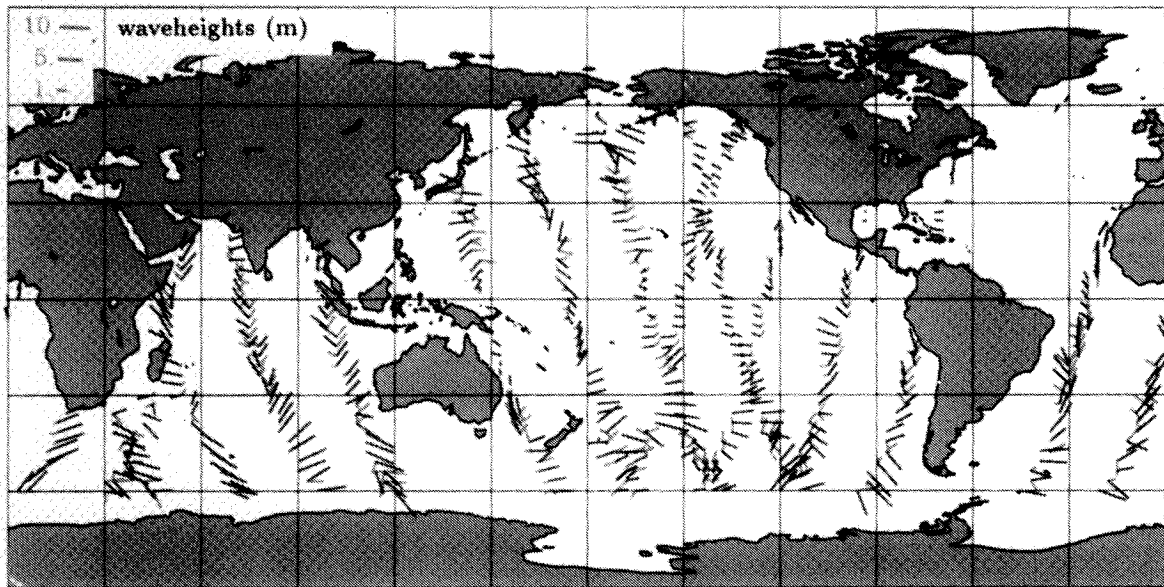


Figure 3b: Same as Fig. 3a, but for collocated WAM wave model spectra.

Conclusions

Following a pilot study using data obtained for January 22-24, 1992, global ERS-1 SAR wave mode data have been routinely processed in Hamburg since July 1992. The wave spectra extracted from the SAR image spectra, provided in the Fast Delivery Product format by ESTEC, show excellent overall agreement with wave spectra computed with the operational ECMWF WAM wave model. The significant wave heights inferred from the SAR-derived wave spectra, which were calibrated independently of the SAR calibration against the measured clutter spectra, are of comparable accuracy to the ERS-1 radar altimeter wave height measurements. Individual wave systems, quantified using a modified version of Gerling's partitioning scheme, are resolved in detail in both the model and the SAR-derived spectra and also show good overall agreement. Nevertheless, systematic differences can be identified for individual wave systems, indicating errors in the analyzed wind fields or possibly in the wave model physics. It is anticipated that the planned assimilation of the detailed wave spectral information from the ERS-1 SAR wave mode data in wave models will lead to significantly improved wave and wind field analyses and forecasts.

Acknowledgment: The authors wish to thank C. Rufenach and W. Alpers for helpful discussions, and B. Hansen, ECMWF, for providing the collocated WAM wave spectra. The paper was supported by the Bundesministerium für Forschung und Technologie, Kontrakt Nr. 01 QS 9014.

References

- Alpers, W., and C. Brüning, 1986, On the relative importance of motion-related contributions to the SAR imaging of ocean surface waves, *IEEE Trans. Geosci. Remote Sens.*, GE-24, 873-885.
- Hasselmann, K., R. K. Raney, W. J. Plant, W. Alpers, R. A. Shuchman, D. R. Lzenga, C. L. Rufenach, and M. J. Tucker, 1985, Theory of SAR ocean wave imaging, a MARSEN view, *J. Geophys. Res.*, 90, 4659-4686.
- Brüning, C., W. Alpers, and K. Hasselmann, 1990, Monte-Carlo simulation studies of the nonlinear imaging of a two dimensional surface wave field by a synthetic aperture radar, *Int. J. Remote Sens.*, 11, 10, 1695-1727.
- Hasselmann, K., S. Hasselmann, C. Brüning, and A. Speidel, 1991, Interpretation and application of SAR wave image spectra in wave models, In *Directional Ocean Wave Spectra*. Edited by Robert C. Beal. The Johns Hopkins University Press.
- Hasselmann, K., and S. Hasselmann, 1991, On the non-linear mapping of an ocean wave spectrum into a SAR image spectrum and its inversion, *J. Geophys. Res.*, 96, C6, 10713-10729.
- Krogstad, H. E., 1992, A simple derivation of Hasselmann's non-linear ocean-synthetic aperture radar transform, *J. Geophys. Res.*, 97, 2421-2425.
- Alpers, W., and K. Hasselmann, 1982, Spectral signal to clutter and thermal noise properties of ocean wave imaging synthetic aperture radars, *Int. J. Remote Sens.*, GE-24, 873-885.
- Brüning, C., S. Hasselmann, K. Hasselmann, S. Lehner, and T. Gerling, 1993, First evaluation of ERS-1 synthetic aperture radar wave mode data, (in preparation).
- Gerling, T., 1992, Partitioning sequences and arrays of directional ocean wave spectra into component wave systems, *J. Atmospheric and Oceanic Techn.*, 9, 4, 444-458.
- WAMDIG: The WAM-Development and Implementation Group, Hasselmann S., K. Hasselmann, E. Bauer, L. Bertotti, C.V. Cardone, J.A. Ewing, J.A. Greenwood, A. Guillaume, P.A.E.M. Janssen, G.J. Komen, P. Lionello, M. Reistad, and L. Zambresky, 1988, The WAM Model - a third generation ocean wave prediction model, *J. Phys. Oceanogr.*, 18, 12, 1775-1810.
- Gower, J.F.R., 1983, "Layover" in satellite radar images of ocean waves, *J. Geophys. Res.*, 88, 7719-7720.
- Hansen, B., and H. Günther, 1992, ERS-1 radar altimeter validation with the WAM model, *Proceedings of the ERS-1 Geophysical Validation Campaign, 27-30 April 1992*, Penhors, Bretagne, France.
- Bauer, E., S. Hasselmann, K. Hasselmann, and H. C. Graber, 1992, Validation and assimilation of Seasat altimeter wave heights using the WAM wave model, *J. Geophys. Res.*, 97, 12671-12682.